Analyst

Accepted Manuscript

ROYAL SOCIETY OF CHEMISTRY

www.rsc.org/analyst

Cite this: DOI: 10.1039/c0xx00000x

www.rsc.org/xxxxxx

ARTICLE TYPE

Designing and Fabricating of Double Resonance Substrate with Metallic Nanoparticles-Metallic Grating Coupling System for Highly Intensified Surface-Enhanced Raman Spectroscopy

Ying Zhou,[a,b] Xuanhua Li,[a] Xingang Ren,[c] Liangbao Yang,[a,b] and Jinhuai Liu[a]

Received (in XXX, XXX) Xth XXXXXXXXX 20XX, Accepted Xth XXXXXXXXX 20XX
DOI: 10.1039/b000000x

Recently, the nanoparticle-film coupling systems that metal nanoparticles (supported localized surface plasmons LSPs) separated from a flat metal film (supported surface plasmon polaritons SPPs) by a spacer have been widely reported due to its strong local enhancement field. However, the rather limited number of works employing design for combing metal grating into the nanoparticle-film gap system. Here, we propose and fabricate a novel double-resonance SERS system through strategically assembling Au NPs spaced by MoO_3 nanospacer from an Ag grating film. The Ag grating showing clear SPP effect is the first time to be used to the double-resonance system and the monolayer Au NPs array is well assembled onto the top of the Ag grating with compact and uniform distribution (inter-particles gap about 5 nm). As a result, we experimentally and theoretically demonstrate a significant near-field enhancement. The very strong near-field produced in the proposed SERS substrates is due to multiple couplings including the Au NPs-Ag grating film coupling and Au NPs-Au NPs coupling. In addition, the as-proposed SERS substrates show good reproducibility of SERS, which will become potential application in the plasmonic sensing and analytical science in the future.

Introduction

Surface-enhanced Raman scattering (SERS) has been a promising and powerful analytical technique since its discovery.[1,2] It refers to the phenomenon whereby Raman scattering is significantly enhanced when molecules are adsorbed on metallic nanostructures.[3] There have been many debates regarding its origin to be electromagnetic or chemical. According to the widely accepted compromise, the SERS is mainly caused by the electromagnetic contribution.[4-7]

Surface plasmons (SPs) are a collective oscillation of electrons at the boundaries between materials and are often categorized into two classes: surface plasmon polaritons (SPPs) and localized surface plasmons (LSPs).[8] SPPs are propagating electromagnetic waves bound to the interfaces between metals and dielectrics. They can be excited on a metal surface by prism coupling or by grating coupling over a large range of frequencies. LSPs, on the other hand, are nonpropagating excitations of the electrons in metal nanoparticles (NPs) that are much smaller than the incident wavelength. The LSP resonance properties of a metal nanoparticle depend on its size, shape, the permittivity and the dielectric environment.[9] These phenomena can lead to strong electromagnetic field enhancement near the nanostructure surfaces, and this has been employed for SERS.[10-18] Theoretical studies have predicted that strong coupling between LSPs and SPPs occurs when their resonance frequencies are approximately equal.[19-22]

Recently, the nanoparticle-film coupling systems that metal nanoparticles (supported localized surface plasmons LSPs) separated from a flat metal film (supported surface plasmon polaritons SPPs) by a spacer have been widely reported due to its strong local enhancement field. One of the interesting features of NPs-film coupling configuration is that it is compatible, at least for most of its construction, which can be popularly adopted in most of typical analytical sciences and the related fields, such as surface-enhanced Raman scattering (SERS), surface-enhanced fluorescence spectra, and other plasmonic sensing with requirements of large area and great spot-to-spot uniformity.[23-26] In the work of Chu,[23] the design includes a metallic nano-disk array separated from a gold film by a dielectric spacer. The SPP on the gold film interacts with the LSPR of the metallic array and double resonance characteristics are observed in optical transmission measurements. In the work of Banaee,[24] "in-plane" nano-particle pairs are used to obtain the plasmonic coupling.

Metal grating structure is a famous structure, which shows efficient SPP. There are many reports about taking advantage of SPP effect from metal grating in plasmonic sensing and analytical science. Unfortunately, there are just a handful of reports about studying the double plasmonic effect with metal NPs supported by metal grating structures. In this work, we propose and fabricate a novel double-resonance SERS system through strategically assembling Au NPs spaced by MoO_3 nanospacer from an Ag grating film. The Ag grating showing clear SPP effect is the first time to be used to the double-resonance system and the monolayer Au NPs array is well assembled onto the top of the Ag grating with compact and uniform distribution (inter-particles gap about 5 nm). As a result, we experimentally and theoretically demonstrate a significant near-field enhancement (the experimental enhancement factor reaches to 2.47×10^7, which is one of the highest reported to date in the double-resonance system). The very strong near-field produced in the proposed SERS substrates is due to multiple couplings including the Au

NPs-Ag grating film coupling and Au NPs-Au NPs coupling. In addition, the as-proposed SERS substrates show good reproducibility of SERS, which will become potential application in the plasmonic sensing and analytical science in the future.

Experimental

Synthesis of SERS substrates

1. Fabrication of Ag grating: PDMS, prepared by mixing an oligomer (Silard 184, Dow corning) and a curing agent (10:1, v/v), was poured onto the silicon nanograting master. After removing the air bubbles and thermally curing at 79 ℃ for 3-4 h, PDMS molds were obtained in which the grating of the periodic nanostructures corresponded to the dimension of the master grating. Silver (80 nm) layers and MoO_3 spacer with different thickness were thermally evaporated onto the PDMS grating mold, in a vacuum at 10^{-6} Torr, respectively.

2. Fabrication of Au nanoparticles: The synthesis of Au NPs was performed using the chemical reduction of chloroauric acid with sodium citrate method introduced by Frens.[27] $HAuCl_4$ solution (1.0 mL, 1.0 wt%) was mixed with water (99.0 mL) and heated to boiling point. Upon boiling, trisodium citrate tetrahydrate (1.3 mL, 1.0 wt%) was added quickly to induce particle formation, during prolonged heating under reflux for 30 min. The Au NPs with a diameter of 25 nm were obtained. The synthesis of Au monolayer film was described by gold nanoparticle assembly approach previously developed by Zhou.[28] A solution of 1×10^{-6} M mPEG-SH in deionized water was first prepared. The appropriate polymeric solution was added to 2.94×10^{-6} M colloidal Au NPs. The sample was kept for about 8 h at room temperature under stirring. Finally, the solution was assembled onto a substrate, and close-packed NPs could be easily obtained.

SERS and Raman experiments

The SERS data is collected on a LabRAM HR800 confocal microscope Raman system (Horiba JobinYvon) using a He-Ne ion laser operating at 632.85 nm. The laser beam was focused on the sample in a size of about 1.5 μm using a ×50 LMPLFLN microscope objective. The laser power was approximately 1mW and the integration time was 1s for each spectrum. The data is collected with the same accumulation and integration times for all samples. We drip the crystal violet (CV) solutions on the substrates, and after they are dry, the substrates were subjected to SERS measurements. We collected SERS spectra from several randomly selected positions on the substrates.

Theoretical modeling

Maxwell's equations were rigorously solved utilizing the finite-difference time-domain (FDTD) method to better understand the nature of the strong near-field enhancement in the Au NPs-Ag grating coupling system.[29,30] In modeling, the sample geometries closely match to those of the actual experimental samples, i.e., a 25 nm Au NP on a Ag grating with 350 nm period separated by a MoO_3. The thickness of MoO_3 is tuned from 2 nm, 15 nm, 30 nm, and 70 nm, respectively. The gap between neighboring Au NPs is about 5 nm. The complex dielectric constant of metallic Au was taken from Johnson and Chrity.[31]

Results and Discussion

Double resonance substrate fabrication and design

A schematic diagram of the double resonance SERS substrate is shown in Scheme 1. It consists of a gold nanoparticle array, a MoO_3 spacer and a continuous silver grating film. PDMS mold was firstly prepared, followed by thermally evaporating silver layers and MoO_3 spacer onto the PDMS grating mold, respectively. The period of grating is 350 nm, as shown in Fig. 1A. Considering that local field enhancement of hot spots are critically sensitive to the spacer between the nanoparticle and the metal film, we will study the effect of thickness of MoO_3 to the SERS enhancement by fabricating four substrates with different the thickness of MoO_3 spacer (2 nm, 15 nm, 35 nm, 70 nm.)

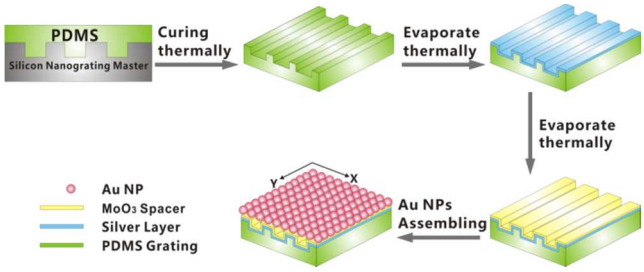

Scheme 1 Schematic representation of the synthesis of Au NPs/MoO_3/Ag grating double resonance substrate. Actual device has hundreds of periods along x and y axes; only a small portion of it depicted here.

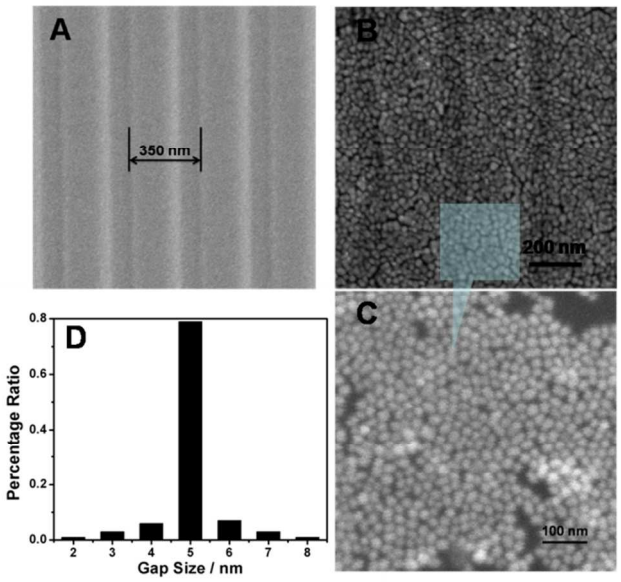

Fig. 1 (A) SEM image of Ag grating with 350 nm period. (B) SEM image of Au NPs distributed on Ag grating. (C) SEM image of Au NPs distributed on Si wafer. (D) The statistical analysis of the gap size distributions of Au NPs.

After placing the MoO_3 film onto the surface of Ag grating, we will consider how to place Au NPs onto the surface of MoO_3 covered Ag grating. Here, we conduct our own-a very simple and versatile nanoscale force induced gold nanoparticle assembly approach to form the ordered monolayer Au NPs array (see Fig. 1C).[28] Actually, if we cannot find an effective way to well arrange the Au NPs on the top of the grating, we will encounter many problems, especially in SERS measurement, such as poor reproducibility of the SERS-active sites. Since LSPR is highly dependent on the spacing between nanoparticles, a nanoparticle array with uniform shapes and size distributions provide the largest SERS enhancement. Fig. 1B shows the SEM image of the as-proposed Au NPs-Ag grating coupling system after an monolayer Au NPs array finally is fabricated by our own self-assembly method on the top of the MoO_3 spacer. The Au NPs (25 nm) covered on the Ag grating surface is distributing compactly and uniformly, shows to be a promising substrate for high-reproducibility SERS detection. Especially, the interparticle gap

(about 5 nm gap, which was clearly revealed by the statistical analysis of the gap size distribution, as shown in Fig. 1D, more details can be seen in Fig. S1) is very small, which will be benefit for the NP-NP coupling to generate gigantic plasmonic enhancement. Since there are four grating with different spacer thickness, so we obtain four kinds of double resonance substrates. For simple reading hereinafter, we name the double resonance substrate using grating with 2 nm thick MoO_3 spacer as sample 1, the substrate using grating with 15 nm, 35 nm, 70 nm thick MoO_3 spacer as sample 2, sample 3, and sample 4, respectively. So the gold nanoparticles of the fabricated device are spheres with diameter of 25 nm and periods of 30 nm. The silver film is 100 nm thick. The thickness of the MoO_3 spacer is varied from 20 nm to 60 nm. The fabricated substrates are illuminated with collimated and polarized laser light at normal incidence. The polarization is parallel to one of the axes of the rectangular lattice, i.e. the x axis in Scheme 1.

SERS measurements

To evaluate the sensitivity of the SERS performance of the double resonance substrates, SERS experiments were conducted using CV as the target molecule owing to its well-established vibrational features. We will first study the effect of thickness of MoO_3 to the SERS performance. After obtain the optimized thickness of MoO_3, we will also evaluate the SERS enhancement performance by comparing the double SERS substrate (Au NPs/MoO_3/Ag grating) with the single SERS substrate including Ag grating and Au NPs. Fig. 2 shows the SERS sensitivity measurement obtained from the double resonance substrates treated in a series of CV with 633 nm excitation. The Raman bands at about 422, 804, 913, 1174, 1368, and 1620 cm^{-1} can be attributed to CV and agree well with literature data.[32] With decreasing CV concentration, the intensity of the Raman peaks become gradually weakened. Raman peaks can be obtained even in 10^{-9} concentration of CV, which means that the double resonance substrates can keep its sensitivity for SERS detection when the concentration of CV is greater than 10^{-9} M. It displays the outstanding SERS sensitivity of the substrates. Furthermore, we study the enhancement of the four Au NPs-Ag grating coupling system with different MoO_3 thickness by calculate their enhancement factor (EF) (see Table 1).[33-37] Assuming that the excitation volume as a cylinder, the diameter (d) and the height (h) of the laser spot were determined by the following equations:

$$d = \frac{1.22\lambda_{laser}}{NA} = 1.54\ \mu m \quad (1)$$

$$h = \frac{2.2n\lambda_{laser}}{\pi(NA)^2} = 2.89\mu m \quad (2)$$

where λ_{laser} is the wavelength of the laser (λ_{laser} = 633 nm), Numerical Aperturec (NA) = 0.5, n is the refractive index of neat CV crystal powder (n ≈ 1.63). The absolute magnitude of the EF for reversible hotspots was estimated according to the following equation:

$$EF = \frac{I_{SERS}/N_{SERS}}{I_{bulk}/N_{bulk}} \quad (3)$$

I_{SERS} and I_{bulk} denote the Raman scattering intensities from the CV adsorbed on the surface of double resonance substrates and the solid CV, respectively. N_{SERS} and N_{bulk} represent the numbers of the corresponding surface and solid molecules effectively excited by the laser beam, respectively. The number of CV molecules excited in the bulk solid, N_{bulk}, can be calculated as following equation (4):

$$N_{bulk} = \frac{\pi(\frac{d}{2})^2 h\rho N_A}{M} \quad (4)$$

Where ρ and M are the density and molecular weight of CV, respectively, N_A represents the Avogadro constant. In this study, the density (1.19 g/cm^3) and molecular weight (407.98 g/mol) of solid CV. The calculated value of N_{bulk} equals to 9.45×10^9. N_{SERS} is the average number of adsorbed molecules in the scattering volume for the SERS measurements. We used 5 μL 1×10^{-9} M CV to evaluate the enhancement factor. In this case, the CV molecules can strongly bind to the Ag surface. We assumed that all CV molecules could adsorb onto the surface of the substrate and all CV molecules were uniformly distributed over the surface. The diameter (D) of the substrate square piece is 2 mm, while the diameter (d) of the laser spot is 1.54 μm (Eqn. 1). Therefore, N_{SERS} can be estimated to be about 10^3.

The test must be under identical experimental conditions (laser wavelength, laser power, microscope objective or lenses, spectrometer, etc.), and for the same preparation conditions. Based on the intensity at 1620 cm^{-1}, we find the sample 1 with 2 nm MoO_3 thickness shows the strongest Raman enhancement. By the way, the calculated EF factor for grating should be orders smaller than SERS enhancement from particle arrays. The reason for not so small SERS observed experimentally on grating could be caused by the rough surfaces of the grating due to thermal evaporation.

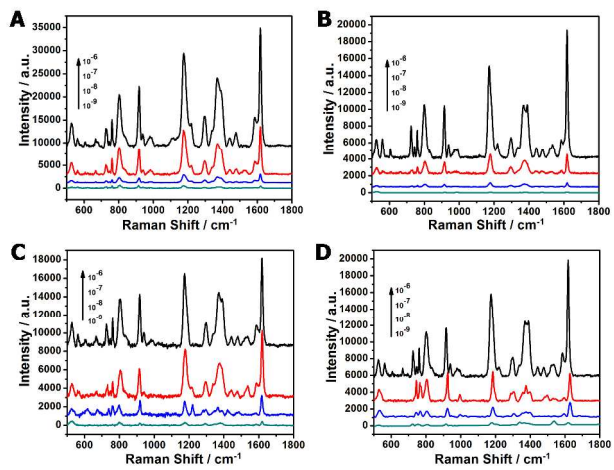

Fig. 2 The SERS spectra of different concentrations of CV solution collected on (A) sample 1, (B) sample 2, (C) sample 3, (D) sample 4.

Substrate	Sample 1	Sample 2	Sample 3	Sample 4	Ag Grating	Au NPs
EF	2.47×10^7	1.36×10^7	9.44×10^6	1.29×10^7	6.58×10^6	2.44×10^6

Table. 1 Calculated SERS Enhancement Factors for double resonance substrates and Au NPs arrays substrate.

Except for studying the effect of MoO_3 thickness in the Au NPs-Ag grating coupling system, we also compare SERS signals obtained from the double plasmonic structure (Au NPs-Ag grating coupling system) to single Ag grating or single Au NPs structure exhibiting single resonance. Fig. 3A shows the SERS spectra obtained from the samples (Ag grating, Au NPs array, sample 1, sample 2, sample 3, sample 4) treated in 1×10^{-6} M CV with 633 nm excitation. It can be found that the SERS signals of CV obtained from double resonance substrates are all stronger than that obtained from single resonance substrates, and sample 1

arrives at the highest degree. The SERS enhancement intensity from sample 1 substrate at 1620 cm^{-1} (about 26000) is eleven times stronger than that from Au NPs (about 2300), which gives the weakest enhancement. It turned out that the SERS spectra obtained from the samples treated in 1×10^{-7}, 1×10^{-8}, 1×10^{-9} M CV demonstrate the same outcome as Fig. 3A, the SERS signal obtained from composite substrates exhibiting double resonance behavior are all stronger than that obtained from Au NPs exhibiting single resonance, and sample 1-the substrate with spacer thickness of 2 nm shows the highest enhancement. As shown in Table 1, the double resonance structures can provide roughly 11 times larger enhancement than single resonance only "Au NPs array" structures. The experimental EF reaches to 2.47×10^{7}, which is one of the highest reported to date in the double-resonance system. The very strong near-field produced in the proposed SERS substrates is due to multiple couplings including the Au NPs-Ag grating film coupling and Au NPs-Au NPs coupling (will be discussed by our theoretical modelling later). In addition, to our best knowledge, the Ag grating showing clear SPP effect is the first time to be used to the double-resonance system and the monolayer Au NPs array is well assembled onto the top of the Ag grating with compact and uniform distribution. Although previous study about NPs-planar film system achieve great successes, limitations in achieving double-resonance SERS system through strategically assembling Au NPs spaced by MoO_3 nanospacer from an Ag grating film still exist. Our current study by conducting a very simple and versatile nanoscale force induced gold nanoparticle assembly approach to form the ordered monolayer Au NPs array on the top of grating surface can directly address the issues. As a result, the results clearly indicate that the Au NPs-Ag grating coupling system with 2 nm MoO_3 spacer dramatically boosts the intensity of Raman scattering and, therefore, has the potential to become a powerful tool in analytical science and the related fields.

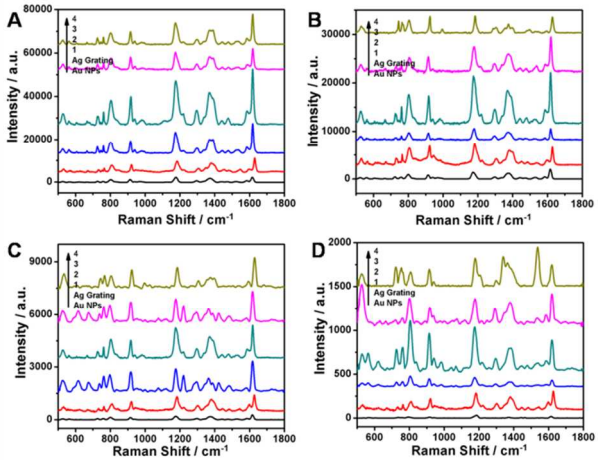

Fig. 3 SERS spectra of (A) 1×10-6M, (B) 1×10-7 M, (C) 1×10-8 M, (D) 1×10-9 M CV molecules obtained from sample 1, sample 2, sample 3, sample 4 and Ag grating, Au NPs array substrates.

Why sample1 substrate shows the highest SERS enhancement? As shown in scheme 2, a surface plasmon is a quantum of an electron concentration wave that can exist at a dielectric–metal interface. The surface plasmon propagates along the metal surface and decays exponentially into both media. Thus the excited surface plasmons from the Ag surface can be transferred to the top metal (Au) surface through the dielectric layer. The thinner the dielectric layer is, the less surface plasmon decays. Accordingly, the conduction electrons on the Au surface are further localized. We conclude that the variation in coupling coefficient vs spacer thickness for the double resonance structure arises from the dependence of the efficiency with which SPPs on an Ag grating film are excited by an array of scatterers on the distance from the scatterers to the film.

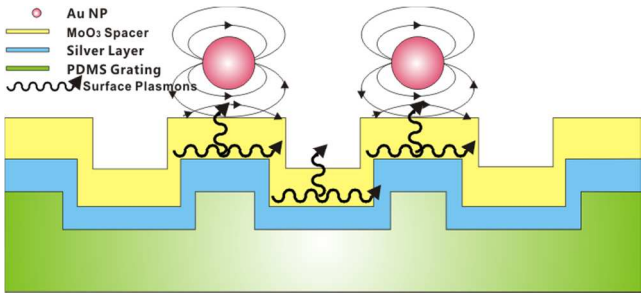

Scheme 2 Schematic of the fabricated double resonance substrate showing high SERS enhancement.

FDTD simulations

To better understand the nature of the strong near-field enhancement in the Au NPs-Ag grating coupling system, we have conducted a theoretical study utilizing the finite-difference time-domain (FDTD) method on the system in which the optical interactions between Au NPs themselves as well as between Au NPs and Ag grating have been fully considered. In modeling, the sample geometries closely match to those of the actual experimental samples, i.e., a 25 nm Au NP on an Ag grating with 350 nm period separated by different thickness of MoO_3 spacer (2 nm, 15 nm, 35 nm, 70 nm). The gap between neighboring Au NPs is about 5 nm. We first simulate the near field spectra for the single resonance and double resonance structure. Fig. 4 shows the cross-section near field profiles of TM polarized light at 633 nm for different metal structures: (a) Au NPs-Au NPs coupling with 5 nm, (b) Single Ag grating, (c) double-resonance Au NP/MoO_3/Ag Grating and (d) partial enlargement of Au NP/MoO_3/Ag grating. For the Au NPs array structure, we find the (plasmonic-induced) strong near-field with local enhancement factor (EF) of 9.21×10^{6} where EF is approximately defined as $|E_{local}/E_0|^4$. The strong near field located at the NP-NP gap is because of the strong plasmonic coupling (Fig. 4A). In contrast, for the single Ag grating structure, the evanescent field above the Ag grating indicates the excitation of the SPP mode on the interface of the Ag film and the MoO_3 spacer (Fig. 4B) and the local EF is 5.24×10^{7}. For the Au NP/MoO_3/Ag grating double-resonance structure, enhanced near fields in the vicinity of the gold nanoparticle can be seen(Fig. 4C, 4D), but with the addition of an extended evanescent field above the Ag grating, which is the character of the SPP. These results indicate that the two resonances for strong coupling case carry both the characters of LSPs and SPPs and finally the local EF reach to 8.38×10^{8}.

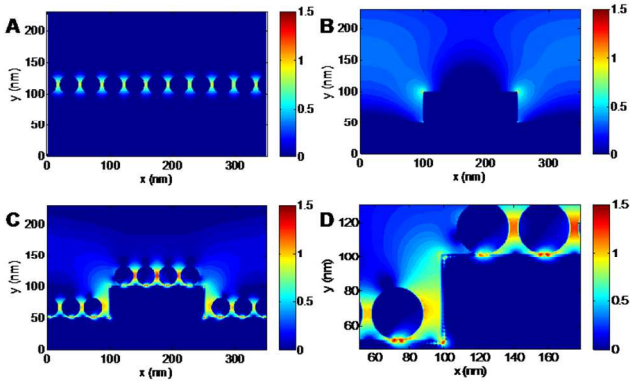

Fig. 4 The cross-section near field profiles of TM polarized light at 633 nm for different metalstructures: (A) Au NPs-NPs coupling with 5 nm, (B) Single Ag grating and (C) double-resonance Au NP/MoO_3/Ag grating, (D) partial enlargement of Au NP/MoO_3/Ag grating.

Then we simulate the cross-section near field profiles for double-resonance Au NP/MoO_3/Ag grating structure with different thickness of MoO_3, as shown in Fig. 5. It can be seen that, enhanced near fields exist around the gold nanoparticles and an extended evanescent field is above the Ag grating. We observe that the Au NP/MoO_3/Ag grating structure with 2 nm thick MoO_3 shows the highest field enhancement. We also observe that the stronger plasmonic enhancement is, the smaller the thickness of MoO_3 spacer between the upper Au NPs and lower Ag grating is. Our result is consistent with the previous report that the local field enhancement of hot spots is critically sensitive to the nanoscale spacer between the NP and the film.[38]

As a consequence, our experimental and theoretical results reveal a greater field enhancement for Au NPs-Ag grating coupling system due to the multiple couplings including Au NPs-Au NPs coupling and Au NPs-Ag grating coupling, which will play very important role in the Au NPs-Ag grating system. On one hand, the multiple couplings considerably strengthen the near-field. Thus enormous EF of 2.47×10^7 has been achieved. On the other hand, the very strong field enhancement at system can also offers a unique opportunity in highly sensitive analyte characterization.

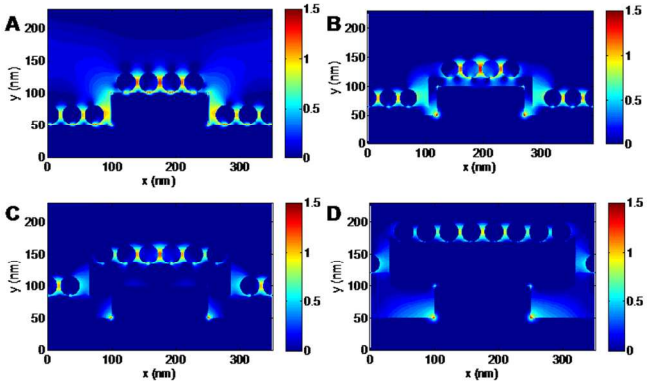

Fig. 5 The cross-section near field profiles of TM polarized light at 633 nm for double-resonance Au NP/MoO_3/Ag grating structure with different thickness of MoO_3: (A) 2 nm, (B) 15 nm, (C) 35 nm, and (D) 70 nm.

Reproducibility of SERS detection

When employing SERS technology, the reproducibility of SERS substrates should be taken into account. The relative standard deviation (RSD) of major peaks is often used to estimate the reproducibility of SERS signals. The main Raman vibrations of CV at 1174, 1368, 1620 cm^{-1} were obviously enhanced at all spots indicating excellent SERS activity and reproducibility. Fig. 6 shows the SERS-RSD spectrum of CV molecules, randomly collected from 50 positions of the sample 1substrate. The RSD of the Raman vibrations from the sample 1substrate at 1174, 1368, and 1620cm^{-1} are 14.94, 13.54, and 14.96%, respectively. The maximal RSD value of signal intensities of major SERS peaks is observed to be below 0.2, indicating that the double resonance substrate has a good reproducibility across the entire area.[39] The compact and uniform distribution of Au NPs on the Ag grating surface is the reason of why the double resonance substrate shows high-reproducibility SERS detection.

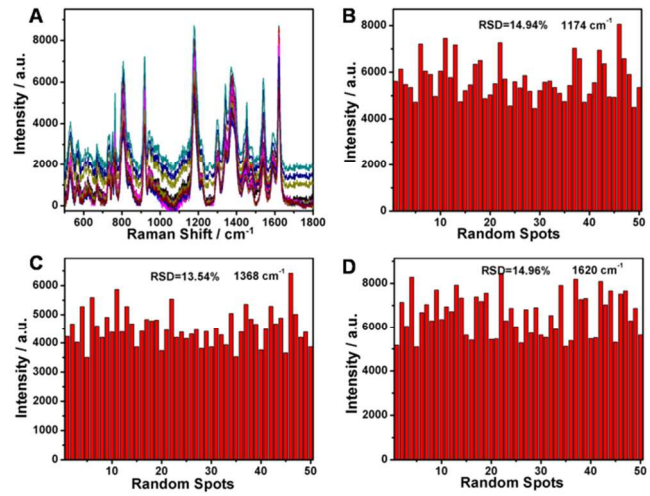

Fig. 6 (A) Series of SERS spectra of 10^{-6} M CV collected on randomly from 50 spots of the sample 1 substrate. (B), (C) and (D) are the intensities of the main vibrations of 10^{-6} M CV for the 1174, 1368 and 1620 cm^{-1}.

Conclusions

We have proposed a novel NPs-Film coupling system by introducing Ag grating in this system. Our results show that the Au NPs-Ag grating coupling system offers tremendous near-field enhancement with one of the highest enhancement ratio (2.47×10^7) reported to date in the NPs-film coupling system. The Ag grating showing clear SPP effect is the first time to be used to the double-resonance system and the monolayer Au NPs array is well assembled onto the top of the Ag grating with compact and uniform distribution (inter-particles gap about 5 nm).Our experimental and theoretical results show that the enhancement can be explained due to the multiple couplings between Ag NPs as well as between the Ag film and Ag NPs. By studying organic dye CV as an analyte, we show that the as-proposed Au NPs-Ag grating coupling system can be used to realize very sensitive detection of most of environmental pollutants. Furthermore, we strongly believe that this simple and reliable method would offer stepping stones for enabling quantitative plasmonic sensing at single molecule level. Our results show that the proposed system can function as a powerful tool in analytical science and the related fields.

Notes and references

[a] *Institute of Intelligent Machines, Chinese Academy of Sciences, Hefei, 230031, China. Fax: (+86)551-5592420; E-mail: lbyang@iim.ac.cn, jhliu@iim.ac.cn, Ying zhou and Xuanhua Li contributed equally to this work.*
[b] *School of Chemistry and Chemical Engineering, Anhui University, Hefei, 230039, China.*
[c] *Key Lab of Intelligent Computing and Signal Processing, Anhui University, Hefei, 230039, China.*
† Electronic Supplementary Information (ESI) available:

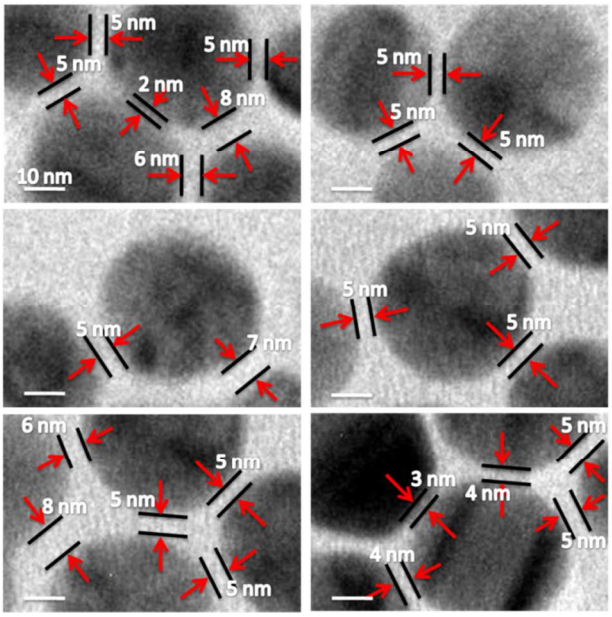

Fig. S1 Typical higher-magnification TEM images and the specific measurements of Au NPs gap distance distribution of interparticle separations.

See DOI: 10.1039/b000000x/

‡ Footnotes should appear here. These might include comments relevant to but not central to the matter under discussion, limited experimental and spectral data, and crystallographic data.

1 D. L. Jeanmaire and R. P. Van Duyne, *J. Electroanal. Chem.*, 1977, **84**, 1-20.
2 M. G. Albrecht and J. A. Creighton, *J. Am. Chem. Soc.*, 1977, **99**, 5215-5217.
3 K. Kneipp, M.Moskovits and H.Kneipp, *Springer: NewYork*, 2007.
4 A. Campion and P. Kambhampati, *Chem. Soc. Rev.*, 1998, **27**, 241-250.
5 C. L. Haynes, A. D. McFarland and R. P. Van Duyne, *Anal. Chem.*, 2005, **77**, 338A-346A.
6 P. L. Stiles, J. A. Dieringer, N. C. Shah and R. R. Van Duyne, *Annu. Rev. Anal. Chem.*, 2008, **1**, 601-626.
7 M. Moskovits, *Rev. Mod. Phys.*, 1985, **57**, 783-826.
8 S. A. Maier, *Springer*, 2007.
9 K. L. Kelly, E. Coronado, L. L. Zhao and G. C. Schatz, *J. Phys. Chem. B*, 2003, **107**, 668-677.
10 K. Kneipp, Y. Wang, H. Kneipp, L. T. Perelman, I. Itzkan, R. R. Dasari and M. S. Feld, *Phys. Rev. Lett.*, 1997, **78**, 1667-1670.
11 K. Kneipp, H. Kneipp, I. Itzkan, R. R. Dasari and M. S. Feld, *J. Phys. Condens. Matter.*, 2002, **14**, R597-R624.
12 A. D. McFarland, M. A. Young, J. A. Dieringer and R. P. Van Duyne, *J. Phys. Chem. B*, 2005, **109**, 11279-11285.
13 C. E. Talley, J. B. Jackson, C. Oubre, N. K. Grady, C. W. Hollars, S. M. Lane, T. R. Huser, P. Nordlander, and N. J. Halas, *Nano Lett.*, 2005, **5**, 1569-1574.
14 T. H. Reilly, S. H. Chang, J. D. Corbman, G. C. Schatz, and K. L. Rowlen, *J. Phys. Chem. C*, 2007, **111**, 1689-1694.
15 C. L. Haynes, A. D. McFarland and R. P. Van Duyne, *Anal. Chem.*, 2005, **77**, 338A-346A.
16 H. X. Xu, E. J. Bjerneld, M. Käll and L. Börjesson, *Phys. Rev. Lett.*, 1999, **83**, 4357-4360.
17 H. X. Xu, J. Aizpurua, M. Käll and P. Apell, *Phys. Rev. E*, 2000, **62**, 4318-4324.
18 M. Kahl and E. Voges, *Phys. Rev. B*, 2000, **61**, 14078-14088.
19 N. Papanikolaou, *Phys. Rev. B*, 2007, **75**, 235426.
20 A. Ghoshal and P. G. Kik, *J. Appl. Phys.*, 2008, **103**, 113111.
21 Y. Z. Chu and K. B. Crozier, *IEEE Lasers and Electro-Optics Society*, 2008, 492-493.
22 Y. Z. Chu and K. B. Crozier, *Opti. Lett.*, 2009, **34**, 244-246.
23 Y. Z. Chu, M. G. Banaee and K. B. Crozier, *Acs Nano*, 2010, **4**, 2804-2810.
24 M. G. Banaee and K. B. Crozier, *ACS Nano*, 2011, **5**, 307-314.
25 A. Q. Chen, R. L. Miller, A. E. DePrince III, A. Joshi-Imre, E. Shevchenko, L. E. Ocola, S. K. Gray, U. Welp and V. K. Vlasko-Vlasov, *Small*, 2013, **9**, 1939-1946.
26 D. X. Wang, W. Q. Zhu, Y. Z. Chu and K. B. Crozier, *Adv. Mater.,* 2012, **24**, 4376-4380.
27 G. Frens, *Nature-Phys Sci*., 1973, **241**, 20-22.
28 X. Zhou, F. Zhou, H. L. Liu, L. B. Yang and J. H. Liu, *Analyst*, 2013, **138**, 5832-5838.
29 X. G. Ren, Z. X. Huang, X. L. Wu, S. L. Lu, H. Wang, L. Wu and S. Li, *Comput. Phys. Commun.*, 2012, **183**, 1192-1200.
30 A. Taflove and S. C. Hagness, *Artech House: Boston*, 2005.
31 P. B. Johnson and R. W. Christy, *Phys. Rev. B*, 1972, **6**, 4370-4379.
32 M. V. Canamares, C. Chenal, R. L. Birke and J. R. Lombardi, *J. Phys. Chem. C*, 2008, **112**, 20295-20300.
33 G. Hong, C. Li and L. Qi, *Adv. Funct. Mater.*, 2010, **20**, 3774-3783.
34 E. C. Le Ru, E. Blackie, M. Meyer and P. G. Etchegoin, *J. Phys. Chem. C*, 2007, **111**, 13794-13803.
35 X. M. Lin, Y. Cui, Y. H. Xu, B. Ren and Z. Q. Tian, *Anal. Bioanal. Chem.*, 2009, **394**, 1729-1745.
36 S. Tian, Q. Zhou, Z. Gu, X. Gu and J. Zheng, *Analyst*, 2013, **138**, 2604-2612.
37 H. L. Liu, Y. D. Sun, Z. Jin, L. B. Yang and J. H. Liu, *Chem. Sci.*, 2013, **4**, 3490-3496.
38 C. Ciraci, R. T.Hill, J. J. Mock, Y. Urzhumov, A. I. Fernandez-Dominguez, S. A. Maier, J. B. Pendry, A. Chilkoti and D. R. Smith, *Science*, 2012, **337**, 1072-1074.
39 B. H. Zhang, H. S. Wang. L. H. Lu, K. L. Ai, G. Zhang and X. L. Cheng, *Adv. Funct. Mater.*, 2008, **18**, 2348-2355.